Search for a High-Mass Diphoton State and Limits on Randall-Sundrum Gravitons at CDF

T. Aaltonen,[23] A. Abulencia,[24] J. Adelman,[13] T. Affolder,[10] T. Akimoto,[55] M.G. Albrow,[17] S. Amerio,[43] D. Amidei,[35] A. Anastassov,[52] K. Anikeev,[17] A. Annovi,[19] J. Antos,[14] M. Aoki,[55] G. Apollinari,[17] T. Arisawa,[57] A. Artikov,[15] W. Ashmanskas,[17] A. Attal,[3] A. Aurisano,[53] F. Azfar,[42] P. Azzi-Bacchetta,[43] P. Azzurri,[46] N. Bacchetta,[43] W. Badgett,[17] A. Barbaro-Galtieri,[29] V.E. Barnes,[48] B.A. Barnett,[25] S. Baroiant,[7] V. Bartsch,[31] G. Bauer,[33] P.-H. Beauchemin,[34] F. Bedeschi,[46] S. Behari,[25] G. Bellettini,[46] J. Bellinger,[59] A. Belloni,[33] D. Benjamin,[16] A. Beretvas,[17] J. Beringer,[29] T. Berry,[30] A. Bhatti,[50] M. Binkley,[17] D. Bisello,[43] I. Bizjak,[31] R.E. Blair,[2] C. Blocker,[6] B. Blumenfeld,[25] A. Bocci,[16] A. Bodek,[49] V. Boisvert,[49] G. Bolla,[48] A. Bolshov,[33] D. Bortoletto,[48] J. Boudreau,[47] A. Boveia,[10] B. Brau,[10] L. Brigliadori,[5] C. Bromberg,[36] E. Brubaker,[13] J. Budagov,[15] H.S. Budd,[49] S. Budd,[24] K. Burkett,[17] G. Busetto,[43] P. Bussey,[21] A. Buzatu,[34] K. L. Byrum,[2] S. Cabrera[q],[16] M. Campanelli,[20] M. Campbell,[35] F. Canelli,[17] A. Canepa,[45] S. Carrillo[i],[18] D. Carlsmith,[59] R. Carosi,[46] S. Carron,[34] B. Casal,[11] M. Casarsa,[54] A. Castro,[5] P. Catastini,[46] D. Cauz,[54] M. Cavalli-Sforza,[3] A. Cerri,[29] L. Cerrito[m],[31] S.H. Chang,[28] Y.C. Chen,[1] M. Chertok,[7] G. Chiarelli,[46] G. Chlachidze,[17] F. Chlebana,[17] I. Cho,[28] K. Cho,[28] D. Chokheli,[15] J.P. Chou,[22] G. Choudalakis,[33] S.H. Chuang,[52] K. Chung,[12] W.H. Chung,[59] Y.S. Chung,[49] M. Cilijak,[46] C.I. Ciobanu,[24] M.A. Ciocci,[46] A. Clark,[20] D. Clark,[6] M. Coca,[16] G. Compostella,[43] M.E. Convery,[50] J. Conway,[7] B. Cooper,[31] K. Copic,[35] M. Cordelli,[19] G. Cortiana,[43] F. Crescioli,[46] C. Cuenca Almenar[q],[7] J. Cuevas[l],[11] R. Culbertson,[17] J.C. Cully,[35] S. DaRonco,[43] M. Datta,[17] S. D'Auria,[21] T. Davies,[21] D. Dagenhart,[17] P. de Barbaro,[49] S. De Cecco,[51] A. Deisher,[29] G. De Lentdecker[c],[49] G. De Lorenzo,[3] M. Dell'Orso,[46] F. Delli Paoli,[43] L. Demortier,[50] J. Deng,[16] M. Deninno,[5] D. De Pedis,[51] P.F. Derwent,[17] G.P. Di Giovanni,[44] C. Dionisi,[51] B. Di Ruzza,[54] J.R. Dittmann,[4] M. D'Onofrio,[3] C. Dörr,[26] S. Donati,[46] P. Dong,[8] J. Donini,[43] T. Dorigo,[43] S. Dube,[52] J. Efron,[39] R. Erbacher,[7] D. Errede,[24] S. Errede,[24] R. Eusebi,[17] H.C. Fang,[29] S. Farrington,[30] I. Fedorko,[46] W.T. Fedorko,[13] R.G. Feild,[60] M. Feindt,[26] J.P. Fernandez,[32] R. Field,[18] G. Flanagan,[48] R. Forrest,[7] S. Forrester,[7] M. Franklin,[22] J.C. Freeman,[29] I. Furic,[13] M. Gallinaro,[50] J. Galyardt,[12] J.E. Garcia,[46] F. Garberson,[10] A.F. Garfinkel,[48] C. Gay,[60] H. Gerberich,[24] D. Gerdes,[35] S. Giagu,[51] P. Giannetti,[46] K. Gibson,[47] J.L. Gimmell,[49] C. Ginsburg,[17] N. Giokaris[a],[15] M. Giordani,[54] P. Giromini,[19] M. Giunta,[46] G. Giurgiu,[25] V. Glagolev,[15] D. Glenzinski,[17] M. Gold,[37] N. Goldschmidt,[18] J. Goldstein[b],[42] A. Golossanov,[17] G. Gomez,[11] G. Gomez-Ceballos,[33] M. Goncharov,[53] O. González,[32] I. Gorelov,[37] A.T. Goshaw,[16] K. Goulianos,[50] A. Gresele,[43] S. Grinstein,[22] C. Grosso-Pilcher,[13] R.C. Group,[17] U. Grundler,[24] J. Guimaraes da Costa,[22] Z. Gunay-Unalan,[36] C. Haber,[29] K. Hahn,[33] S.R. Hahn,[17] E. Halkiadakis,[52] A. Hamilton,[20] B.-Y. Han,[49] J.Y. Han,[49] R. Handler,[59] F. Happacher,[19] K. Hara,[55] D. Hare,[52] M. Hare,[56] S. Harper,[42] R.F. Harr,[58] R.M. Harris,[17] M. Hartz,[47] K. Hatakeyama,[50] J. Hauser,[8] C. Hays,[42] M. Heck,[26] A. Heijboer,[45] B. Heinemann,[29] J. Heinrich,[45] C. Henderson,[33] M. Herndon,[59] J. Heuser,[26] D. Hidas,[16] C.S. Hill[b],[10] D. Hirschbuehl,[26] A. Hocker,[17] A. Holloway,[22] S. Hou,[1] M. Houlden,[30] S.-C. Hsu,[9] B.T. Huffman,[42] R.E. Hughes,[39] U. Husemann,[60] J. Huston,[36] J. Incandela,[10] G. Introzzi,[46] M. Iori,[51] A. Ivanov,[7] B. Iyutin,[33] E. James,[17] D. Jang,[52] B. Jayatilaka,[16] D. Jeans,[51] E.J. Jeon,[28] S. Jindariani,[18] W. Johnson,[7] M. Jones,[48] K.K. Joo,[28] S.Y. Jun,[12] J.E. Jung,[28] T.R. Junk,[24] T. Kamon,[53] P.E. Karchin,[58] Y. Kato,[41] Y. Kemp,[26] R. Kephart,[17] U. Kerzel,[26] V. Khotilovich,[53] B. Kilminster,[39] D.H. Kim,[28] H.S. Kim,[28] J.E. Kim,[28] M.J. Kim,[17] S.B. Kim,[28] S.H. Kim,[55] Y.K. Kim,[13] N. Kimura,[55] L. Kirsch,[6] S. Klimenko,[18] M. Klute,[33] B. Knuteson,[33] B.R. Ko,[16] K. Kondo,[57] D.J. Kong,[28] J. Konigsberg,[18] A. Korytov,[18] A.V. Kotwal,[16] A.C. Kraan,[45] J. Kraus,[24] M. Kreps,[26] J. Kroll,[45] N. Krumnack,[4] M. Kruse,[16] V. Krutelyov,[10] T. Kubo,[55] S. E. Kuhlmann,[2] T. Kuhr,[26] N.P. Kulkarni,[58] Y. Kusakabe,[57] S. Kwang,[13] A.T. Laasanen,[48] S. Lai,[34] S. Lami,[46] S. Lammel,[17] M. Lancaster,[31] R.L. Lander,[7] K. Lannon,[39] A. Lath,[52] G. Latino,[46] I. Lazzizzera,[43] T. LeCompte,[2] J. Lee,[49] J. Lee,[28] Y.J. Lee,[28] S.W. Lee[o],[53] R. Lefèvre,[20] N. Leonardo,[33] S. Leone,[46] S. Levy,[13] J.D. Lewis,[17] C. Lin,[60] C.S. Lin,[17] M. Lindgren,[17] E. Lipeles,[9] A. Lister,[7] D.O. Litvintsev,[17] T. Liu,[17] N.S. Lockyer,[45] A. Loginov,[60] M. Loreti,[43] R.-S. Lu,[1] D. Lucchesi,[43] P. Lujan,[29] P. Lukens,[17]

G. Lungu,[18] L. Lyons,[42] J. Lys,[29] R. Lysak,[14] E. Lytken,[48] P. Mack,[26] D. MacQueen,[34] R. Madrak,[17] K. Maeshima,[17] K. Makhoul,[33] T. Maki,[23] P. Maksimovic,[25] S. Malde,[42] S. Malik,[31] G. Manca,[30] A. Manousakis[a],[15] F. Margaroli,[5] R. Marginean,[17] C. Marino,[26] C.P. Marino,[24] A. Martin,[60] M. Martin,[25] V. Martin[g],[21] M. Martínez,[3] R. Martínez-Ballarín,[32] T. Maruyama,[55] P. Mastrandrea,[51] T. Masubuchi,[55] H. Matsunaga,[55] M.E. Mattson,[58] R. Mazini,[34] P. Mazzanti,[5] K.S. McFarland,[49] P. McIntyre,[53] R. McNulty[f],[30] A. Mehta,[30] P. Mehtala,[23] S. Menzemer[h],[11] A. Menzione,[46] P. Merkel,[48] C. Mesropian,[50] A. Messina,[36] T. Miao,[17] N. Miladinovic,[6] J. Miles,[33] R. Miller,[36] C. Mills,[10] M. Milnik,[26] A. Mitra,[1] G. Mitselmakher,[18] A. Miyamoto,[27] S. Moed,[20] N. Moggi,[5] B. Mohr,[8] C.S. Moon,[28] R. Moore,[17] M. Morello,[46] P. Movilla Fernandez,[29] J. Mülmenstädt,[29] A. Mukherjee,[17] Th. Muller,[26] R. Mumford,[25] P. Murat,[17] M. Mussini,[5] J. Nachtman,[17] A. Nagano,[55] J. Naganoma,[57] K. Nakamura,[55] I. Nakano,[40] A. Napier,[56] V. Necula,[16] C. Neu,[45] M.S. Neubauer,[9] J. Nielsen[n],[29] L. Nodulman,[2] O. Norniella,[3] E. Nurse,[31] S.H. Oh,[16] Y.D. Oh,[28] I. Oksuzian,[18] T. Okusawa,[41] R. Oldeman,[30] R. Orava,[23] K. Osterberg,[23] C. Pagliarone,[46] E. Palencia,[11] V. Papadimitriou,[17] A. Papaikonomou,[26] A.A. Paramonov,[13] B. Parks,[39] S. Pashapour,[34] J. Patrick,[17] G. Pauletta,[54] M. Paulini,[12] C. Paus,[33] D.E. Pellett,[7] A. Penzo,[54] T.J. Phillips,[16] G. Piacentino,[46] J. Piedra,[44] L. Pinera,[18] K. Pitts,[24] C. Plager,[8] L. Pondrom,[59] X. Portell,[3] O. Poukhov,[15] N. Pounder,[42] F. Prakoshyn,[15] A. Pronko,[17] J. Proudfoot,[2] F. Ptohos[e],[19] G. Punzi,[46] J. Pursley,[25] J. Rademacker[b],[42] A. Rahaman,[47] V. Ramakrishnan,[59] N. Ranjan,[48] I. Redondo,[32] B. Reisert,[17] V. Rekovic,[37] P. Renton,[42] M. Rescigno,[51] S. Richter,[26] F. Rimondi,[5] L. Ristori,[46] A. Robson,[21] T. Rodrigo,[11] E. Rogers,[24] S. Rolli,[56] R. Roser,[17] M. Rossi,[54] R. Rossin,[10] P. Roy,[34] A. Ruiz,[11] J. Russ,[12] V. Rusu,[13] H. Saarikko,[23] A. Safonov,[53] W.K. Sakumoto,[49] G. Salamanna,[51] O. Saltó,[3] L. Santi,[54] S. Sarkar,[51] L. Sartori,[46] K. Sato,[17] P. Savard,[34] A. Savoy-Navarro,[44] T. Scheidle,[26] P. Schlabach,[17] E.E. Schmidt,[17] M.P. Schmidt,[60] M. Schmitt,[38] T. Schwarz,[7] L. Scodellaro,[11] A.L. Scott,[10] A. Scribano,[46] F. Scuri,[46] A. Sedov,[48] S. Seidel,[37] Y. Seiya,[41] A. Semenov,[15] L. Sexton-Kennedy,[17] A. Sfyrla,[20] S.Z. Shalhout,[58] M.D. Shapiro,[29] T. Shears,[30] P.F. Shepard,[47] D. Sherman,[22] M. Shimojima[k],[55] M. Shochet,[13] Y. Shon,[59] I. Shreyber,[20] A. Sidoti,[46] P. Sinervo,[34] A. Sisakyan,[15] A.J. Slaughter,[17] J. Slaunwhite,[39] K. Sliwa,[56] J.R. Smith,[7] F.D. Snider,[17] R. Snihur,[34] M. Soderberg,[35] A. Soha,[7] S. Somalwar,[52] V. Sorin,[36] J. Spalding,[17] F. Spinella,[46] T. Spreitzer,[34] P. Squillacioti,[46] M. Stanitzki,[60] A. Staveris-Polykalas,[46] R. St. Denis,[21] B. Stelzer,[8] O. Stelzer-Chilton,[42] D. Stentz,[38] J. Strologas,[37] D. Stuart,[10] J.S. Suh,[28] A. Sukhanov,[18] H. Sun,[56] I. Suslov,[15] T. Suzuki,[55] A. Taffard[p],[24] R. Takashima,[40] Y. Takeuchi,[55] R. Tanaka,[40] M. Tecchio,[35] P.K. Teng,[1] K. Terashi,[50] J. Thom[d],[17] A.S. Thompson,[21] E. Thomson,[45] P. Tipton,[60] V. Tiwari,[12] S. Tkaczyk,[17] D. Toback,[53] S. Tokar,[14] K. Tollefson,[36] T. Tomura,[55] D. Tonelli,[46] S. Torre,[19] D. Torretta,[17] S. Tourneur,[44] W. Trischuk,[34] S. Tsuno,[40] Y. Tu,[45] N. Turini,[46] F. Ukegawa,[55] S. Uozumi,[55] S. Vallecorsa,[20] N. van Remortel,[23] A. Varganov,[35] E. Vataga,[37] F. Vazquez[i],[18] G. Velev,[17] C. Vellidis[a],[46] G. Veramendi,[24] V. Veszpremi,[48] M. Vidal,[32] R. Vidal,[17] I. Vila,[11] R. Vilar,[11] T. Vine,[31] M. Vogel,[37] I. Vollrath,[34] I. Volobouev[o],[29] G. Volpi,[46] F. Würthwein,[9] P. Wagner,[53] R.G. Wagner,[2] R.L. Wagner,[17] J. Wagner,[26] W. Wagner,[26] R. Wallny,[8] S.M. Wang,[1] A. Warburton,[34] D. Waters,[31] M. Weinberger,[53] W.C. Wester III,[17] B. Whitehouse,[56] D. Whiteson[p],[45] A.B. Wicklund,[2] E. Wicklund,[17] G. Williams,[34] H.H. Williams,[45] P. Wilson,[17] B.L. Winer,[39] P. Wittich[d],[17] S. Wolbers,[17] C. Wolfe,[13] T. Wright,[35] X. Wu,[20] S.M. Wynne,[30] A. Yagil,[9] K. Yamamoto,[41] J. Yamaoka,[52] T. Yamashita,[40] C. Yang,[60] U.K. Yang[j],[13] Y.C. Yang,[28] W.M. Yao,[29] G.P. Yeh,[17] J. Yoh,[17] K. Yorita,[13] T. Yoshida,[41] G.B. Yu,[49] I. Yu,[28] S.S. Yu,[17] J.C. Yun,[17] L. Zanello,[51] A. Zanetti,[54] I. Zaw,[22] X. Zhang,[24] J. Zhou,[52] and S. Zucchelli[5]

(CDF Collaboration*)

[1] *Institute of Physics, Academia Sinica, Taipei, Taiwan 11529, Republic of China*

[2] *Argonne National Laboratory, Argonne, Illinois 60439*

[3] *Institut de Fisica d'Altes Energies, Universitat Autonoma de Barcelona, E-08193, Bellaterra (Barcelona), Spain*

[4] *Baylor University, Waco, Texas 76798*

[5] *Istituto Nazionale di Fisica Nucleare, University of Bologna, I-40127 Bologna, Italy*

[6] *Brandeis University, Waltham, Massachusetts 02254*

[7] *University of California, Davis, Davis, California 95616*

[8] *University of California, Los Angeles, Los Angeles, California 90024*

[9] University of California, San Diego, La Jolla, California 92093
[10] University of California, Santa Barbara, Santa Barbara, California 93106
[11] Instituto de Fisica de Cantabria, CSIC-University of Cantabria, 39005 Santander, Spain
[12] Carnegie Mellon University, Pittsburgh, PA 15213
[13] Enrico Fermi Institute, University of Chicago, Chicago, Illinois 60637
[14] Comenius University, 842 48 Bratislava, Slovakia; Institute of Experimental Physics, 040 01 Kosice, Slovakia
[15] Joint Institute for Nuclear Research, RU-141980 Dubna, Russia
[16] Duke University, Durham, North Carolina 27708
[17] Fermi National Accelerator Laboratory, Batavia, Illinois 60510
[18] University of Florida, Gainesville, Florida 32611
[19] Laboratori Nazionali di Frascati, Istituto Nazionale di Fisica Nucleare, I-00044 Frascati, Italy
[20] University of Geneva, CH-1211 Geneva 4, Switzerland
[21] Glasgow University, Glasgow G12 8QQ, United Kingdom
[22] Harvard University, Cambridge, Massachusetts 02138
[23] Division of High Energy Physics, Department of Physics,
University of Helsinki and Helsinki Institute of Physics, FIN-00014, Helsinki, Finland
[24] University of Illinois, Urbana, Illinois 61801
[25] The Johns Hopkins University, Baltimore, Maryland 21218
[26] Institut für Experimentelle Kernphysik, Universität Karlsruhe, 76128 Karlsruhe, Germany
[27] High Energy Accelerator Research Organization (KEK), Tsukuba, Ibaraki 305, Japan
[28] Center for High Energy Physics: Kyungpook National University,
Taegu 702-701, Korea; Seoul National University, Seoul 151-742,
Korea; SungKyunKwan University, Suwon 440-746, Korea
[29] Ernest Orlando Lawrence Berkeley National Laboratory, Berkeley, California 94720
[30] University of Liverpool, Liverpool L69 7ZE, United Kingdom
[31] University College London, London WC1E 6BT, United Kingdom
[32] Centro de Investigaciones Energeticas Medioambientales y Tecnologicas, E-28040 Madrid, Spain
[33] Massachusetts Institute of Technology, Cambridge, Massachusetts 02139
[34] Institute of Particle Physics: McGill University, Montréal,
Canada H3A 2T8; and University of Toronto, Toronto, Canada M5S 1A7
[35] University of Michigan, Ann Arbor, Michigan 48109
[36] Michigan State University, East Lansing, Michigan 48824
[37] University of New Mexico, Albuquerque, New Mexico 87131
[38] Northwestern University, Evanston, Illinois 60208
[39] The Ohio State University, Columbus, Ohio 43210
[40] Okayama University, Okayama 700-8530, Japan
[41] Osaka City University, Osaka 588, Japan
[42] University of Oxford, Oxford OX1 3RH, United Kingdom
[43] University of Padova, Istituto Nazionale di Fisica Nucleare,
Sezione di Padova-Trento, I-35131 Padova, Italy
[44] LPNHE, Universite Pierre et Marie Curie/IN2P3-CNRS, UMR7585, Paris, F-75252 France
[45] University of Pennsylvania, Philadelphia, Pennsylvania 19104
[46] Istituto Nazionale di Fisica Nucleare Pisa, Universities of Pisa,
Siena and Scuola Normale Superiore, I-56127 Pisa, Italy
[47] University of Pittsburgh, Pittsburgh, Pennsylvania 15260
[48] Purdue University, West Lafayette, Indiana 47907
[49] University of Rochester, Rochester, New York 14627
[50] The Rockefeller University, New York, New York 10021
[51] Istituto Nazionale di Fisica Nucleare, Sezione di Roma 1,
University of Rome "La Sapienza," I-00185 Roma, Italy
[52] Rutgers University, Piscataway, New Jersey 08855
[53] Texas A&M University, College Station, Texas 77843
[54] Istituto Nazionale di Fisica Nucleare, University of Trieste/ Udine, Italy
[55] University of Tsukuba, Tsukuba, Ibaraki 305, Japan
[56] Tufts University, Medford, Massachusetts 02155
[57] Waseda University, Tokyo 169, Japan
[58] Wayne State University, Detroit, Michigan 48201
[59] University of Wisconsin, Madison, Wisconsin 53706
[60] Yale University, New Haven, Connecticut 06520

We have performed a search for new particles which decay to two photons using 1.2 fb^{-1} of integrated luminosity from $p\bar{p}$ collisions at $\sqrt{s} = 1.96$ TeV collected using the CDF II Detector at

the Fermilab Tevatron. We find the diphoton mass spectrum to be in agreement with the standard model expectation, and set limits on the cross section times branching ratio for the Randall-Sundrum graviton, as a function of diphoton mass. We subsequently derive lower limits for the graviton mass of 230 GeV/c^2 and 850 GeV/c^2, at the 95% confidence level, for coupling parameters ($k/\overline{M}_{Pl}$) of 0.01 and 0.1 respectively.

PACS numbers: 12.38.Qk 13.85.Rm 13.85.Qk

A potential signature for new, heavy particles is a narrow mass resonance decaying to two energetic photons. Such a signature could arise from extra spatial dimensions, as in the Randall-Sundrum (RS) model [1]. In this Letter we present the results of the search for this signature in $p\bar{p}$ collision data from the CDF II Detector at the Fermilab Tevatron.

Some string theories propose that as many as seven new spatial dimensions may exist, with their geometry potentially responsible for the apparent weakness of gravity (the hierarchy problem). In the minimal RS model, this geometry is a five-dimensional space with negative curvature, bounded by two three-dimensional, spatially extended membranes (or 'branes'). These branes are separated by a distance πr_c, where r_c is the compactification radius. Using ϕ as the coordinate of the extra dimension ($0 \leq \phi \leq \pi$), the standard model (SM) particles are confined to the "TeV" brane, located at $\phi = \pi$, while the gravitational wavefunction is localized at $\phi = 0$. The scale of physical phenomena on the TeV brane is specified by $\Lambda_\pi = \overline{M}_{Pl}\ e^{-kr_c\pi}$, where $\overline{M}_{Pl} = M_{Pl}/\sqrt{8\pi} = 2.4 \times 10^{18}$ GeV is the effective four-dimensional (reduced) Planck scale and k is a curvature parameter of the order of the Planck scale.

To remove the hierarchy between gravity and the electroweak force, Λ_π is set to approximately 1 TeV. The Planck scale then arises from the small overlap of the graviton wave function with the TeV brane in the fifth dimension, and the compactification scale gives rise to a Kaluza Klein tower of graviton states, an infinite set of four-dimensional particles with increasing masses. This mass spectrum is given by $m_n = x_n(k/\overline{M}_{Pl})\Lambda_\pi$, where x_n are the roots of the first-order Bessel function, and the states couple with strength $1/\Lambda_\pi$. Thus, the widths and masses of the resonances are dependent on the parameter $k/\overline{M}_{Pl}$.

The values of k must be large enough to be consistent with the apparent weakness of gravity, but small enough to prevent the theory from becoming non-perturbative [2]. Given these considerations, we examine values in the range $0.01 < k/\overline{M}_{Pl} < 0.1$. For this range, graviton production results in a diphoton mass peak narrower than the CDF detector resolution. The spin-2 nature of the graviton, decaying by either s- or p-wave states, favors searches in the diphoton channel, where the branching ratio is twice that of any single dilepton channel.

Existing lower mass limits on RS gravitons from a search using the DØ detector, in the combined diphoton, dielectron, and dimuon channels, are 250 GeV/c^2 for $k/\overline{M}_{Pl} = 0.01$ and 785 GeV/c^2 for $k/\overline{M}_{Pl} = 0.1$ at the 95% confidence level (C.L.) [3]. The previous limits from the CDF collaboration are from a combined dielectron and dimuon search, with limits of 170 GeV/c^2 and 710 GeV/c^2 for $k/\overline{M}_{Pl} = 0.01$ and 0.1 respectively [4].

This search uses 1.2 fb^{-1} of integrated luminosity collected by the CDF II Detector operating at $\sqrt{s} = 1.96$ TeV. The detector [5] is approximately forward-backward and azimuthally symmetric. A seven-layer (eight-layer in the forward region) silicon tracker [6] is surrounded by an open-cell drift chamber (COT) [7]. The fiducial coverage of the COT is $|\eta| < 1.0$, and the silicon detector extends the tracking coverage to $|\eta| < 2.0$. The integrated tracking system is contained within a superconducting solenoid, providing a 1.4 T magnetic field. Surrounding these are the electromagnetic and hadronic calorimeters [8], divided into "central" ($|\eta| < 1.1$) and "plug" ($1.1 < |\eta| < 3.6$) regions, providing measurements of both shower energy and position. At the approximate electromagnetic shower maximum, the calorimeters contain fine-grained detectors [9] that measure the shower shape and centroid position in the two dimensions transverse to the shower

*With visitors from [a]University of Athens, 15784 Athens, Greece, [b]University of Bristol, Bristol BS8 1TL, United Kingdom, [c]University Libre de Bruxelles, B-1050 Brussels, Belgium, [d]Cornell University, Ithaca, NY 14853, [e]University of Cyprus, Nicosia CY-1678, Cyprus, [f]University College Dublin, Dublin 4, Ireland, [g]University of Edinburgh, Edinburgh EH9 3JZ, United Kingdom, [h]University of Heidelberg, D-69120 Heidelberg, Germany, [i]Universidad Iberoamericana, Mexico D.F., Mexico, [j]University of Manchester, Manchester M13 9PL, England, [k]Nagasaki Institute of Applied Science, Nagasaki, Japan, [l]University de Oviedo, E-33007 Oviedo, Spain, [m]University of London, Queen Mary College, London, E1 4NS, England, [n]University of California Santa Cruz, Santa Cruz, CA 95064, [o]Texas Tech University, Lubbock, TX 79409, [p]University of California, Irvine, Irvine, CA 92697, [q]IFIC(CSIC-Universitat de Valencia), 46071 Valencia, Spain,

development. Surrounding these detectors is a system of muon detectors [10]. Three levels of real-time trigger systems are used to filter events.

The collision events recorded for analysis were selected by at least one of four triggers. Two of the triggers require two clusters of electromagnetic energy [5]: one of these triggers requires both clusters to have transverse energy $E_T > 12$ GeV, and to be isolated in the calorimeter; while the other requires the two clusters to have $E_T > 18$ GeV, but makes no isolation requirement. To ensure very high trigger efficiency at the largest photon E_T, events are also accepted from two single-photon triggers. The first of these triggers requires $E_T > 50$ GeV without an isolation criterion; the second requires $E_T > 70$ GeV, without an isolation ctriteria, and relaxed requirements on the hadronic energy associated with cluster. The combination of these triggers is effectively 100% efficient for the kinematic region used in this search for diphoton events above a mass of 50 GeV/c^2.

The triggered events are required to have been recorded while the relevant detector elements were fully operational. Events are examined in which either both photons are in the central calorimeter (approximately in the region $|\eta| < 1.04$), or one photon is in the central and the other is in the plug calorimeter (over the region $1.2 < |\eta| < 2.8$). The data were collected between February, 2002 and February, 2006 and correspond to an integrated luminosity of 1.2 fb^{-1} for the central-central (CC) diphoton sample and 1.1 fb^{-1} for the central-plug (CP) sample. The luminosity of the CP sample is reduced because good silicon detector conditions are required for tracking in the plug region.

In both the CC and CP cases, each of the two photons is required to produce a highly electromagnetic energy cluster with $E_T > 15$ GeV and together to have a reconstructed diphoton invariant mass greater than 30 GeV/c^2. Both are required to be in the fiducial region of the shower maximum detectors and to pass the following photon identification requirements: transverse shower profiles consistent with a single photon, additional transverse energy in the calorimeter in a cone of angular radius R = $\sqrt{(\Delta\phi)^2 + (\Delta\eta)^2} = 0.4$ around the photon candidate < 2 GeV, and the scalar sum of the transverse momentum p_T of the tracks in the same cone < 2 GeV/c. Photons in the central detector are required to produce isolated energy clusters in the shower maximum detector.

The selected data consist of 11, 088 CC and 20, 933 CP events. The diphoton invariant mass distribution for these events, histogrammed in bins equivalent to the mass resolution (approximated by $0.13\sqrt{m(\mathrm{GeV}/c^2)} \oplus 0.014m$ GeV, where m is diphoton mass) is shown in Fig. 1. The highest mass pairs occur at 602 GeV/c^2 for the CC data and 454 GeV/c^2 for the CP data, as shown in Fig. 2.

The expected numbers of RS graviton events, as a function of graviton mass, are estimated using the HERWIG 6.510 event generator [12], with CTEQ5L parton distribution functions (PDFs) [13], and processed by the GEANT 3 based CDF II detector simulation [14]. The combined acceptance and selection efficiency for RS events increases from $0.31 \pm 0.01_{stat}$ for gravitons of mass 200 GeV/c^2 to $0.36 \pm 0.01_{stat}$ for gravitons of mass 1050 GeV/c^2. Final corrections to the efficiency are derived by comparing the measured and Monte Carlo simulated detector response to electrons from Z boson decays, since a pure sample of reconstructed photons is not available, and the characteristics of energy deposited in the calorimeter by electrons are almost indistinguishable from those of photons. The largest systematic uncertainties on the expected number of gravitons arise from the luminosity measurement (6%) and the choice of PDF (4%). The latter uncertainty is determined from the variation in the efficiency when employing different PDF parameterizations.

Most Z bosons that decay to e^+e^- are rejected by requiring no associated tracks; however, approximately 1% of these remain in the CP sample at a mass peak below the search region. There are two other significant components to the diphoton data sample. The first is SM diphoton production, which is estimated with the DIPHOX next-to-leading-order (NLO) Monte Carlo [15] calculation. This program computes a cross section as a function of mass. The mass spectrum is then corrected by an efficiency function derived from a SM diphoton sample generated by PYTHIA [16] and processed through the full detector simulation. The leading systematic uncertainty on this background estimate is approximately 20%, which comes from the variation in the cross section when the renormalization scale, Q^2, is varied in the generation. The second component is jets, consisting of quarks that fragment into a high momentum π^0, which subsequently decays as $\pi^0 \to \gamma\gamma$. The resulting photon showers may overlap, and can pass the photon selection. The diphoton mass distribution of this background is derived from a sample of photon-like jets obtained by loosening the photon selection criteria, then removing the events which pass all the signal selection requirements. The selection of the photon-like jets is varied and the resulting variation in the shape of the mass distribution is approximately 20%. This is the leading systematic

uncertainty on the jet background.

To extrapolate to the highest masses, the mass distributions of the two background sources are fitted to a product of a polynomial and the sum of two (for photon-like jets) or three (for DIPHOX) exponentials. The fit to the photon-like jets includes a contribution from the DIPHOX shape to allow for true diphoton events which appear in this sample. For the signal region background estimate, the DIPHOX distribution is normalized to the NLO cross section predicted by DIPHOX. The jet background shape is normalized to the observed shape in the invariant mass region 30 GeV/c^2 to 100 GeV/c^2 after subtracting the estimated background from SM diphoton production.

Figure 2 shows the observed mass spectra compared to the predictions. This estimate of the background, which shows good agreement with the observation, is only for an *a priori* comparison, and is not used in setting upper limits on a specific production model.

To find the most accurate description of the background for setting limits, we fit the CC and CP mass spectra to a polynomial multiplied by a sum of three components: two exponentials and the DIPHOX shape. The normalization of each component is allowed to float in the fit. This function is used for the background estimate as a function of mass with statistical uncertainties propagated from the fits. DIPHOX systematic uncertainties, as described above, are also propagated.

The background shape is combined with the simulated signal shape in a binned likelihood method, with the contents of the bins treated with Poisson statistics. The likelihood as a function of cross section is given by

$$L(\sigma) = \prod_{i=1}^{N_{bins}} \frac{\mu_i(\sigma)^{N_i^d} e^{-\mu_i(\sigma)}}{N_i^d!} \ , \qquad (1)$$

where

$$\mu_i(\sigma) = \frac{\epsilon \mathcal{L} \sigma N_i^s}{N_{tot}^s} + N_i^b \ . \qquad (2)$$

Here N_i^d, N_i^b and N_i^s are respectively the numbers of observed, background and signal events in bin i, and N_{tot}^s is the total number of signal events passing selection requirements. The parameter ϵ is the total acceptance and efficiency for selecting the events predicted by the model, $\mathcal{L}$ is the integrated luminosity, and σ is the model cross section. Systematic uncertainties are included in the likelihood with a gaussian Bayesian prior.

$k/\overline{M}_{Pl}$	Lower Mass Limit (GeV/c^2)
0.1	850
0.07	784
0.05	694
0.025	500
0.01	230

TABLE I: The 95% C.L. lower limits on the mass of the RS graviton for the specified values of $k/\overline{M}_{Pl}$.

The likelihood function is calculated separately for the CC and CP channels, then a combined likelihood is formed from the product of the two, accounting for the correlations among systematic uncertainties. We obtain a posterior density in σ assuming a uniform prior in σ applying Bayes' Theorem. The 95% C.L. upper limit corresponds to the point below which 95% of the integral of the posterior density lies.

The result is shown in Fig. 3, as a function of graviton mass, along with the theoretical cross section times branching ratio for RS gravitons with $k/\overline{M}_{Pl}$ set to 0.1, 0.07, 0.05, 0.025 and 0.01. The leading-order graviton production cross section is multiplied by a factor of 1.3, to correct for diagrams at higher-order in α_s [17]. From the limit on $\sigma \cdot \mathcal{B}(G \to \gamma\gamma)$, lower mass bounds are obtained for the first excited state of the RS graviton as a function of the parameter $k/\overline{M}_{Pl}$. The 95% C.L. excluded region in the $k/\overline{M}_{Pl}$ and graviton mass plane is displayed in Fig. 4, with the mass limits summarized in Table I.

In conclusion, we have searched for evidence of an anomalous peak in the diphoton mass spectrum using approximately 1.2 fb^{-1} of data collected by the CDF II Detector at the Fermilab Tevatron. Our sample includes events with both photons in the central detector, and events with one photon in the central detector and one in the plug detector. We find no evidence of new physics. We evaluate one model of hypothetical new diphoton production and exclude RS gravitons below masses ranging from 230 GeV/c^2 to 850 GeV/c^2, for a coupling parameter $k/\overline{M}_{Pl}$ of 0.01 to 0.1, at the 95% C.L. This results in a significant improvement, at high mass, over the previous best available limit.

We thank the Fermilab staff and the technical staffs of the participating institutions for their vital contributions. This work was supported by the U.S. Department of Energy and National Science Foundation; the Italian Istituto Nazionale di Fisica Nucleare; the Ministry of Education, Culture,

Sports, Science and Technology of Japan; the Natural Sciences and Engineering Research Council of Canada; the National Science Council of the Republic of China; the Swiss National Science Foundation; the A.P. Sloan Foundation; the Bundesministerium für Bildung und Forschung, Germany; the Korean Science and Engineering Foundation and the Korean Research Foundation; the Science and Technology Facilities Council and the Royal Society, UK; the Institut National de Physique Nucleaire et Physique des Particules/CNRS; the Russian Foundation for Basic Research; the Comisión Interministerial de Ciencia y Tecnología, Spain; the European Community's Human Potential Programme; the Slovak R&D Agency; and the Academy of Finland.

[1] L. Randall and R. Sundrum, Phys. Rev. Lett. **83**, 3370 (1999).
[2] H.Davoudiasl, J. L. Hewett, and T.G. Rizzo, Phys. Rev. Lett. **84**, 2080 (2000).
[3] V. M. Abazov *et al.* (DØ Collaboration), Phys. Rev. Lett. **95**, 091801 (2005).
[4] A. Abulencia *et al.* (CDF Collaboration), Phys. Rev. Lett. **95**, 252001 (2005).
[5] D. Acosta *et al.*, Phys. Rev. D **71**, 032001 (2005). CDF uses a cylindrical coordinate system in which ϕ is the azimuthal angle, r is the radius from the nominal beamline, and $+z$ points along the direction of the proton beam. The pseudorapidity is defined as $\eta = -\ln[\tan(\theta/2)]$, where θ is the polar angle measured from the $+z$ axis. Calorimeter energy (track momentum) measured in the plane transverse to the beam is denoted as E_T (p_T).
[6] A. Sill *et al.*, Nucl. Instrum. Methods A **447**, 1 (2000).
[7] T. Affolder *et al.*, Nucl. Instrum. Methods A **526**, 249 (2004).
[8] L. Balka *et al.*, Nucl. Instrum. Methods A **267**, 272 (1988); S. Bertolucci *et al.*, Nucl. Instrum. Methods A **267**, 301 (1988); M. Albrow *et al.*, Nucl. Instrum. Methods A **480**, 524 (2002).
[9] G. Apollinari *et al.*, Nucl. Instrum. Methods A **412**, 515 (1998).
[10] G. Ascoli *et al.*, Nucl. Instrum. Methods A **268**, 33 (1988).
[11] D. Acosta *et al.*, Phys. Rev. Lett. **94**, 091803 (2005).
[12] G. Marchesini *et al.*, Comput. Phys. Commun. **67**, 465 (1992); G. Corcella *et al.*, J. High Energy Phys. **0101**, 010 (2001); G. Corsella *et al.*, hep-ph/0210213v2 (2005).
[13] J. Pumplin *et al.*, J. High Energy Phys. **0207**, 012 (2002).
[14] CERN Program Library Long Writeup W5013 (1993)
[15] T. Binoth, J. Ph. Guillet, E. Pilon, and M. Werlen, Eur. Phys. J. C **16**, 311 (2000).
[16] T. Sjöstrand *et al.*, Comput. Phys. Commun. **135**, 238 (2001).
[17] P. Mathews, V. Ravindran, K. Sridhar, and W.L. van Neerven, Nucl. Phys. B **713**, 333 (2005).

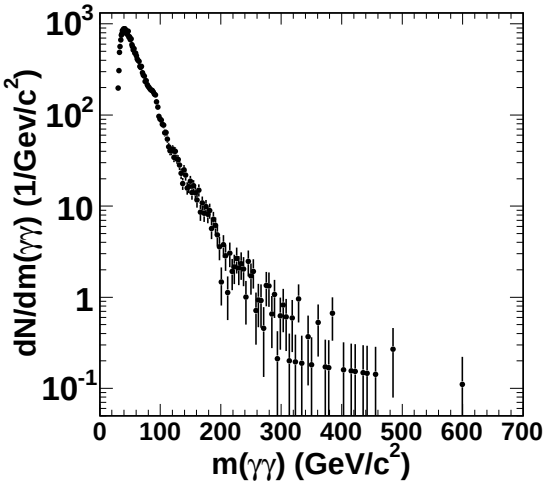

FIG. 1: The diphoton invariant mass distribution of events for both CC and CP channels, histogrammed in bins of approximately one unit of calorimeter mass resolution. The enhancement near 90 GeV/c^2 is due to misidentified Z boson decays to electrons in the CP sample.

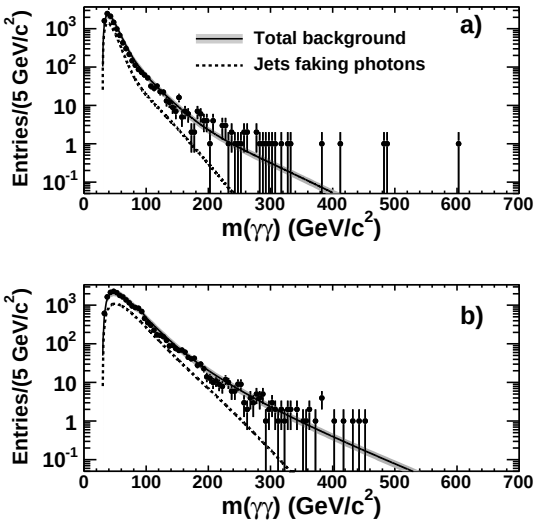

FIG. 2: The mass distribution in the CC (a) and CP (b) signal regions with the *a priori* background overlaid. The points are the data. The dotted line shows the jets which fake photons as predicted from the photon-like jet sample, and the solid line shows this background plus the DIPHOX SM diphoton distribution. The grey band shows the uncertainty on the total background. This background is not used in setting limits.

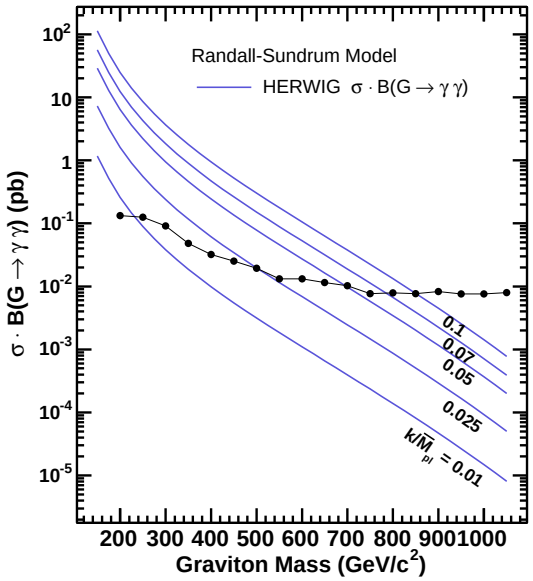

FIG. 3: The 95% C.L. upper limit on the production cross section multiplied by branching fraction of an RS model graviton decaying to diphotons ($\sigma \cdot \mathcal{B}(G \to \gamma\gamma)$), as a function of graviton mass. Also shown are the predicted ($\sigma \cdot \mathcal{B}$) curves for $k/\overline{M}_{Pl} = 0.01$, 0.07, 0.05, 0.025 and 0.1.

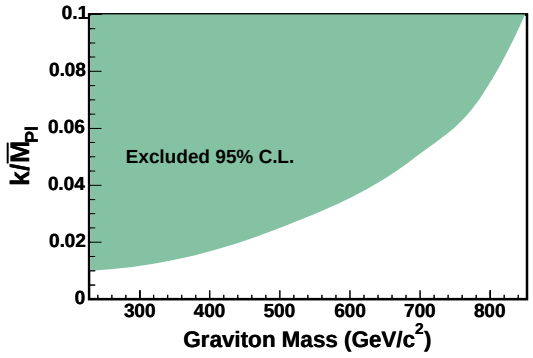

FIG. 4: The 95% C.L. excluded region in the plane of $k/\overline{M}_{Pl}$ and graviton mass.